Supplementary Information: Challenges for DFT: Calculation of CO Adsorption on Electrocatalytically Relevant Metals†

Christianna N. Lininger,[a,b] Joseph A. Gauthier,[a,b] Wan-Lu Li,[a,c] Elliot Rossomme,[c] Valerie Vaissier Welborn,[c,e],Zhou Lin,[a,c] Teresa Head-Gordon,[a,b,c,d] Martin Head-Gordon,[a,c] and Alexis T. Bell[a,b]

S1 Comparison of VASP and Q-Chem

To ensure robustness for the properties computed with VASP, we compared its results to Q-Chem for the metal carbonyl systems for all of the metals we focused on in this study, Au, Ag, Cu, and Pt. For these calculations, we adhere to the Methods outlined in the main text, unless otherwise noted here in the SI. We assessed the differences between properties calculated with Q-Chem and VASP for the energy of adsorption, metal-carbon (M-CO) bond length, carbon-oxygen (MC-O) bond length, and the adsorbed carbon-oxygen harmonic vibrational frequency. To compare the differences between the codes, we calculated the percent difference as (VASP - Q-Chem)/Q-Chem * 100%.

The energies of adsorption between VASP and Q-Chem generally tracked well, and the percent difference between VASP and Q-Chem for the metal-carbon and carbon-oxygen bond lengths are within +/-2% and 1%, respectively, as shown in Figure S1. The change in the C-O bond length upon adsorption to the (111) surfaces between CP2K and VASP also track very well (results not shown). Due to the low percent differences between the MC-O bond lengths between the codes, it is not surprising that the differences for the harmonic vibrational frequencies are also small. To further assess differences in energetics, the dimerization energy of water from the S22 DFT benchmark dataset[2] was computed with Q-Chem and VASP for the same exchange correlation functionals (SCAN, RPBE, and B97M-rV), and acceptable error for H_2O dimerization energy between codes was found and also shown in Fig. S1.

To benchmark the implementation of the B97M-rV functional in VASP and Q-chem, the dissociation energy D_E was computed as the energy of the dimer (Ar-Ar distance of 3.75Å) relative to the energy of the atoms far apart (Ar-Ar distance of 8.00Å). We found a value for -0.2605 kcal/mol for VASP, -0.2565 kcal/mol for Q-Chem, and -0.2786 kcal/mol when compared to a high quality reference calculation[3].

Overall, we found the VASP results to be in good agreement

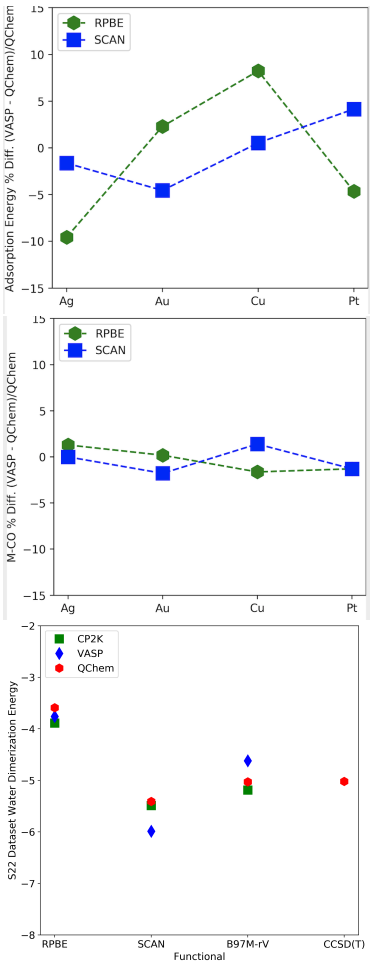

Fig. S1 Percent difference between VASP and Q-Chem for (top) DFT predicted adsorption energy for CO molecule on single M = Au, Ag, Cu, and Pt atoms. (middle) DFT predicted M-CO bond length for the CO molecule on single M = Au, Ag, Cu, and Pt atoms. (bottom) Dimerization energy for water from the S22 DFT benchmark database computed for RPBE, SCAN, and B97M-rV in VASP (blue diamonds) and Q-Chem (red hexagons). A previous reference calculation in CP2K (green squares) is shown for comparison[1]

[a] *Chemical Sciences Division, Lawrence Berkeley National Laboratory, Berkeley, California 94720, USA*
[b] *Department of Chemical and Biomolecular Engineering, University of California, Berkeley, California 94720, USA*
[c] *Kenneth S. Pitzer Center for Theoretical Chemistry, Department of Chemistry, University of California, Berkeley, California 94720, USA*
[d] *Department of Bioengineering, University of California, Berkeley, California 94720, USA*
[e] *Current Address, Virginia Tech, USA*

with Q-Chem results.

S2 Properties calculated with VASP

The DFT calculated bulk metal lattice constants are listed in Table S1 for Ag, Au, Cu, and Pt. Parenthetically following the calculated lattice constant is the percent error from the experimental lattice constant listed in the last column of Table S1.

The equilibrium bond lengths and harmonic vibrational frequencies for the CO molecule are shown in Fig. S2 for each functional compared to the experimental equilibrium bond length and harmonic vibrational frequency.[4]

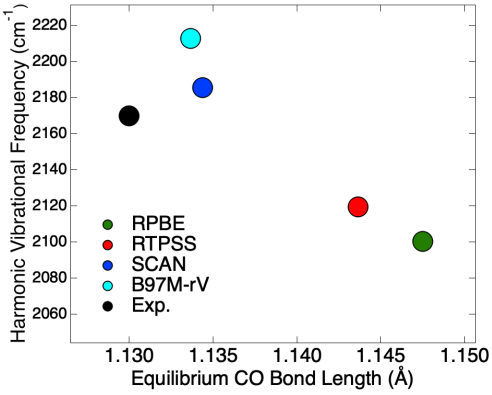

Fig. S2 Theoretically predicted harmonic frequency at the functional determined equilibrium bond length compared to the experimental values (black).

S3 Methods and Data for Molecular Systems

S3.1 Metal Monocarbonyls (MCOs)

In the main text we report and discuss graphical representations of data for binding energies, harmonic vibrational frequencies, and M−C bond lengths for molecular metal monocarbonyls (MCOs). Here, we recapitulate our procedures for these computations and include the numeral data used to generate these plots in the main text.

DFT computations using the RPBE,[5] SCAN,[6], B97M-rV[7], and ωB97X-V[8] density functionals were completed using the Q-Chem package,[9] following previous work.[10] CCSD(T)[11] computations were also performed. Unrestricted wave functions were used in all cases, and solutions were ensured to be stable with respect to mixing of the occupied and virtual orbital spaces. For a given level of correlation, MCO complex geometries were optimized using the def2-TZVPD basis set (Table S2),[12,13] and the absence of imaginary harmonic vibrational frequencies, determined through diagonalization of the full Hessian matrix, were used to confirm that each structure was a minimum. The harmonic vibrational frequencies for these complexes, as well as those for isolated CO at each of the indicated levels of theory, are reported in Table S3.

Single-point energy computations at the def2-TZVPD geometries were completed using the def2-TZVPPD[12,13] and def2-QZVPPD[12,14] basis sets. The def2-QZVPPD energies were taken to approximate the complete basis set (CBS) limit for Hartree-Fock and DFT energies, but a two-point CBS extrapolation scheme was used to determine the limiting behavior of the correlation energy, *viz.*

$$E_{\mathrm{CBS}}(X) = E_X - AX^{-3}, \tag{1}$$

where X is the cardinal number of the basis set, E_{CBS} is the CBS energy, and A is a constant that is determined through comparison of the def2-TZVPPD and def2-QZVPPD results. These numbers were used to calculate CCSD(T) complex binding energies as

$$\Delta E_{\mathrm{bind}} = E^{\mathrm{CBS}}_{\mathrm{MCO}} - E^{\mathrm{CBS}}_{\mathrm{M}} - E^{\mathrm{CBS}}_{\mathrm{CO}}. \tag{2}$$

These results are compared to the analogous def2-QZVPPD binding energies for the present DFT functionals in Table S4.

S3.2 The Water–CO Dimer

The B97M-rV, RPBE, and SCAN density functionals were used to determine the binding energy of the water–CO dimer. Single-point energy computations were performed using the geometry reported by Lique *et al.* (see Table S5).[15] These researchers determined a benchmark CCSD(T)-F12a binding energy with the aug-cc-pVTZ basis set[16] and accounted for the basis set superposition error (BSSE) with the Boys and Bernardi counterpoise correction (CPC) scheme.[17] This computational scheme results in a value that approximates the complete basis set limit for the CCSD(T) binding energy.[15]. Hence, our DFT computations herein employ the def2-QZVPPD basis, which should be approximately complete for this system, and utilize the same BSSE correction as indicated above. We evaluate each of the methods in the present study in reference to the benchmark CCSD(T)-F12a binding energy of $-646.1\,\mathrm{cm}^{-1}$ above and also report ωB97X-V results for comparison.

The data in Table S6 indicate that B97M-rV reproduces the benchmark water–CO binding energy with the most fidelity among the density functionals being evaluated in this paper. Unique among the methods under present consideration, it overbinds the complex by about $28\,\mathrm{cm}^{-1}$. Notably, the percent error of this functional (-4.3%) is of similar magnitude to that for the higher-level ωB97X-V functional (2.9%). The performance of the other DFT functionals deteriorates going to SCAN and finally to RPBE, where the complex is underbound by nearly $200\,\mathrm{cm}^{-1}$ (29.4%). The ability of B97M-rV to reproduce the water–CO binding energy leads to a similar conclusion as many of our other results: B97M-rV is a balanced functional that is well-suited to model the interactions implicated in CO_2R on metal surfaces.

Table S1 Rows 1-4 contain the fully relaxed bulk metal lattice constants for each functional. The experimental values are shown in the final column.

	RPBE	RTPSS	SCAN	B97M-rV	Expt.
Ag	4.23 (+3.5%)	4.12 (+0.7%)	4.08 (-0.2%)	4.10 (+0.3%)	4.09
Au	4.20 (+2.9%)	4.13 (+1.3%)	4.10 (+0.4%)	4.14 (+1.5%)	4.08
Cu	3.68 (+1.7%)	3.60 (-0.5%)	3.56 (-1.5%)	3.53 (-2.4%)	3.62
Pt	4.00 (+1.9%)	3.96 (+0.8%)	3.91 (-0.3%)	3.94 (+0.6%)	3.92

Table S2 M−C bond lengths for MCOs computed using various DFT functionals and CCSD(T). All results obtained using the def2-TZVPD basis set.

Species	B97M-rV	RPBE	SCAN	wB97X-V	CCSD(T)
CuCO	1.921	1.911	1.854	1.963	1.910
AgCO	2.291	2.221	2.123	2.537	2.236
AuCO	2.045	1.951	2.008	2.054	1.979
PtCO	1.770	1.746	1.768	1.782	1.754

Table S3 Harmonic vibrational frequencies of the CO bond for MCOs and free CO computed using various DFT functionals and CCSD(T). All results obtained using the def2-TZVPD basis set.

Species	B97M-rV	RPBE	SCAN	wB97X-V	CCSD(T)
CuCO	2047.9	1945.6	2039.3	2113.6	2071.0
AgCO	2078.0	1954.6	2043.4	2178.0	2079.4
AuCO	2061.5	1953.6	2057.6	2140.2	2067.7
PtCO	2121.0	2026.1	2130.4	2156.2	2091.8
CO	2221.5	2104.1	2211.0	2238.1	2157.5

Table S4 Binding energies (eV) for MCOs computed using various DFT functionals and CCSD(T). DFT results were computed using def2-QZVPPD basis sets, and CCSD(T) results were determined through CBS extrapolation as detailed in the main text and the SI.

Species	B97M-rV	RPBE	SCAN	wB97X-V	CCSD(T)
CuCO	-0.59	-0.61	-0.87	-0.28	-0.35
AgCO	-0.15	-0.11	-0.24	-0.03	-0.02
AuCO	-0.55	-0.66	-1.00	-0.37	-0.58
PtCO	-3.35	-3.51	-4.00	-3.09	-3.58

Table S5 Cartesian coordinates for the water–CO dimer as optimized by Lique *et al.*[15] Distances are reported in atomic units.

Atom	x	y	z
O	0.0000	0.0000	0.1264
H	1.4573	0.0000	-1.0034
H	-1.4573	0.0000	-1.0034
C	5.5391	0.0000	-2.8202
O	7.5860	0.0000	-3.4343

Table S6 Counterpoise corrected binding energies for the water–CO dimer computed using the def2-QZVPPD basis set. Energies are reported in cm^{-1} and percent errors are relative to the computational benchmark value[15] of $-646.1\,\mathrm{cm}^{-1}$.

Method	Binding Energy	Percent Error
ωB97X-v	-627.5	2.9%
B97M-rV	-674.1	-4.3%
RPBE	-456.0	29.4%
SCAN	-592.6	8.3%

Notes and references

1 L. Ruiz Pestana, N. Mardirossian, M. Head-Gordon and T. Head-Gordon, *Chemical Science*, 2017, **8**, 3554–3565.

2 P. Jurečka, J. Šponer, J. Černý and P. Hobza, *Phys. Chem. Chem. Phys.*, 2006, **8**, 1985–1993.

3 D. G. Smith, P. Jankowski, M. Slawik, H. A. Witek and K. Patkowski, *Journal of chemical theory and computation*, 2014, **10**, 3140–3150.

4 K. P. Huber and G. Herzberg, *Molecular Spectra and Molecular Structure*, Springer US, Boston, MA, 1979.

5 B. Hammer, L. B. Hansen and J. K. Nørskov, *Physical Review B - Condensed Matter and Materials Physics*, 1999, **59**, 7413–7421.

6 J. Sun, A. Ruzsinszky and J. Perdew, *Physical Review Letters*, 2015, **115**, 1–6.

7 N. Mardirossian, L. Ruiz Pestana, J. C. Womack, C. K. Skylaris, T. Head-Gordon and M. Head-Gordon, *Journal of Physical Chemistry Letters*, 2017, **8**, 35–40.

8 N. Mardirossian and M. Head-Gordon, *Phys. Chem. Chem. Phys.*, 2014, **16**, 9904–9924.

9 Y. Shao, Z. Gan, E. Epifanovsky, A. T. Gilbert, M. Wormit, J. Kussmann, A. W. Lange, A. Behn, J. Deng, X. Feng, D. Ghosh, M. Goldey, P. R. Horn, L. D. Jacobson, I. Kaliman, R. Z. Khaliullin, T. KuÅ, A. Landau, J. Liu, E. I. Proynov, Y. M. Rhee, R. M. Richard, M. A. Rohrdanz, R. P. Steele, E. J. Sundstrom, H. L. W. III, P. M. Zimmerman, D. Zuev, B. Albrecht, E. Alguire, B. Austin, G. J. O. Beran, Y. A. Bernard, E. Berquist, K. Brandhorst, K. B. Bravaya, S. T. Brown, D. Casanova, C.-M. Chang, Y. Chen, S. H. Chien, K. D. Closser, D. L. Crittenden, M. Diedenhofen, R. A. D. Jr., H. Do, A. D. Dutoi, R. G. Edgar, S. Fatehi, L. Fusti-Molnar, A. Ghysels, A. Golubeva-Zadorozhnaya, J. Gomes, M. W. Hanson-Heine, P. H. Harbach, A. W. Hauser, E. G. Hohenstein, Z. C. Holden, T.-C. Jagau, H. Ji, B. Kaduk, K. Khistyaev, J. Kim, J. Kim, R. A. King, P. Klunzinger, D. Kosenkov, T. Kowalczyk, C. M. Krauter, K. U. Lao, A. D. Laurent, K. V. Lawler, S. V. Levchenko, C. Y. Lin, F. Liu, E. Livshits, R. C. Lochan, A. Luenser, P. Manohar, S. F. Manzer, S.-P. Mao, N. Mardirossian, A. V. Marenich, S. A. Maurer, N. J. Mayhall, E. Neuscamman, C. M. Oana, R. Olivares-Amaya, D. P. OâNeill, J. A. Parkhill, T. M. Perrine, R. Peverati, A. Prociuk, D. R. Rehn, E. Rosta, N. J. Russ, S. M. Sharada, S. Sharma, D. W. Small, A. Sodt, T. Stein, D. StÃŒck, Y.-C. Su, A. J. Thom, T. Tsuchimochi, V. Vanovschi, L. Vogt, O. Vydrov, T. Wang, M. A. Watson, J. Wenzel, A. White, C. F. Williams, J. Yang, S. Yeganeh, S. R. Yost, Z.-Q. You, I. Y. Zhang, X. Zhang, Y. Zhao, B. R. Brooks, G. K. Chan, D. M. Chipman, C. J. Cramer, W. A. G. III, M. S. Gordon, W. J. Hehre, A. Klamt, H. F. S. III, M. W. Schmidt, C. D. Sherrill, D. G. Truhlar, A. Warshel, X. Xu, A. Aspuru-Guzik, R. Baer, A. T. Bell, N. A. Besley, J.-D. Chai, A. Dreuw, B. D. Dunietz, T. R. Furlani, S. R. Gwaltney, C.-P. Hsu, Y. Jung, J. Kong, D. S. Lambrecht, W. Liang, C. Ochsenfeld, V. A. Rassolov, L. V. Slipchenko, J. E. Subotnik, T. V. Voorhis, J. M. Herbert, A. I. Krylov, P. M. Gill and M. Head-Gordon, *Mol. Phys.*, 2015, **113**, 184–215.

10 E. Rossomme, C. N. Lininger, A. T. Bell, T. Head-Gordon and M. Head-Gordon, *Phys. Chem. Chem. Phys.*, 2020, **22**, 781–798.

11 K. Raghavachari, G. W. Trucks, J. A. Pople and M. Head-Gordon, *Chem. Phys. Lett.*, 1989, **157**, 479–483.

12 D. Rappoport and F. Furche, *J. Chem. Phys.*, 2010, **133**, 134105.

13 F. Weigend and R. Ahlrichs, *Phys. Chem. Chem. Phys.*, 2005, **7**, 3297–3305.

14 F. Weigend, F. Furche and R. Ahlrichs, *J. Chem. Phys.*, 2003, **119**, 12753–12762.

15 Y. N. Kalugina, A. Faure, A. van der Avoird, K. Walker and F. Lique, *Phys. Chem. Chem. Phys.*, 2018, **20**, 5469–5477.

16 T. H. Dunning, *J. Chem. Phys.*, 1989, **90**, 1007.

17 S. F. Boys and F. Bernardi, *Mol. Phys.*, 1970, **19**, 553–566.